arXiv:1701.03143v1 [astro-ph.SR] 11 Jan 2017

Journal-Ref: Astronomy Letters, 2014, Vol. 40, No. 6, pp. 334-342

On the nature of the azimuthal asymmetry of protoplanetary disks observed pole-on. The case LkHα 101

T.V. Demidova[1], **V.P. Grinin**[1,2]

1 - Pulkovo Astronomial Observatory of the Russian Academy of Sciences
2 - S. Petersburg State University, V.V. Sobolev Astronomical Institute

e-mail:proxima1@list.ru

Abstract

The model of a protoplanetary disk of a star with a low-mass companion ($M_2 : M_1 \leq 0.1$), moving on a circular orbit, which slightly inclined to the disk plane ($\leq 10^\circ$), is considered. The SPH-method is used to calculate gas-dynamic flows. The motion of the companion on the orbit leads to the inhomogeneous distribution of the matter in the disk: there are a cleared gap, density waves and streams of matter. Because of the disturbances the inner part of the disk is tilted to its periphery and also do not coincides with the orbit plane of the companion. It leads to anisotropic illumination of the disk by the star and, as a consequence, to the appearance of large-scale inhomogeneity on the disk image: it has a bright area in the form of a "horseshoe" and a small shadow zone located asymmetric with respect to the line of nodes. The asymmetry of the disk image is clearly visible even if it is observed pole-on. The motion of the companion on the orbit does not lead to the synchronous movement of the shadow and bright areas: they only make small oscillations relative to the some direction. By using the proposed model we an fairly accurately reproduce the asymmetric image of the disk of star LkHα 101, observed almost pole-on. The study of such asymmetric disks opens up new opportunity for searching massive bodies around young stars.

Keywords: *methods: numerical, protoplanetary disks, planet–disk interactions.*

1 Introduction

In the overwhelming majority of cases the circumstellar disks around young stars are not resolved through a telescope and we know about their existence from circumstantial evidence (intrinsic linear polarization of stars, infrared (IR) excesses, emission line profiles, jets). Optical and IR images of the disks were obtained for dozens of young objects with the Hubble Space Telescope and large ground based telescopes (see, e.g., Padgett et al. 1999; Tuthill et al. 2002; Grady et al. 2005)[1]. In many cases, the quality of these images is already high enough for them to be used to study large-scale features on the disks. Pole-on disks are of particular interest, because for such an orientation, first, the image details are seen better (see, e.g., Hashimoto et al. 2011; Muto et al. 2012). Second, and this is especially important, the images of such disks are affected neither by the anisotropy of light scattering by dust grains nor by the self-shielding of inner disk regions near the dust sublimation zone, which give rise to an asymmetry in the images of the disks if they are inclined relative to the plane of the sky.

The existing methods of observations do not yet allow any planets at their formation stages to be seen in protoplanetary disks. However, their existence can be judged from the distortions in the disk images that they cause during their motion. Hydrodynamic simulations performed by the SPH method (Artymowicz & Lubow 1996; Bate & Bonnell 1997; Sotnikova & Grinin 2007) and by applying finite-difference methods (Günther & Kley 2002; Kaigorodov et al. 2010; Hanawa et al. 2010) show that the motion of a secondary component in a circumstellar disk gives rise to a gap at the disk center, density waves, gas flows, and shock waves. In the models with a low-mass companion ($q < 0.01$), a matter-free ring is formed near the orbital radius of the companion instead of the gap (de Val-Borro et al. 2007). If the companion's orbit is inclined relative to the plane of the circumbinary disk, than the matter captured by the companion from the circumbinary disk forms a disk around the binary's primary component whose plane is inclined both relative to the plane of the outer disk and relative to the orbital plane of the companion (Larwood et al. 1996; Papaloizou & Terquem 1995; Grinin et al. 2010; Demidova et al. 2013; Xiang-Gruess & Papaloizou 2013). It can be seen from Fig. 1b that a global asymmetry in the distribution of matter whose scales are considerably larger than other hydrodynamic inhomogeneities caused by the companion's motion (the companion's accretion disk, the shock waves arising during the collision of gas flows, etc.., which are calculated insufficiently accurately in our SPH models) arises in the circumbinary disk.

The circumstellar disk of β Pic, whose inner region is inclined by several degrees relative to the disk periphery, is an example of such a system. A similar picture is also observed for the Herbig Ae star CQ Tau: the inner part of its circumstellar disk is inclined approximately by $15-20^\circ$ relative to the disk periphery (Eisner et al. 2004; Doucet et al. 2006; Chapillon et al. 2008). Observations of the Rossiter–McLaughlin effect during the transits of planets across the disks of their host stars show that the orbital plane does not coincide with the equatorial plane of the central star for 40% of these objects (see, e.g., Triaud et al. 2010; Albrecht et al. 2012). Possible causes of the appearance of planets and substellar companions in orbits that are noncoplanar with the circumstellar disk have been discussed in recent years in many papers (Papaloizou & Terquem 1995; Lai et al. 2011; Fabrycky & Tremaine 2007; Nagasawa et al. 2008; Thommes & Lissauer 2003; Bate et al. 2010), but the question about the evolution of such binaries still remains unclear (Fragner & Nelson 2010; Bitsch & Kley 2011; Xiang-Gruess & Papaloizou 2013).

The perturbations in the disk caused by the orbital motion of the companion can manifest themselves as periodic circumstellar extinction variations when such binaries are viewed edge-on or at a small angle to the disk plane. The models of such binaries (Demidova et al. 2010; Grinin et al. 2010) well explain the main properties of the cyclic activity of UX Ori stars. Perturbations in the inner regions of the disks also affect the illumination of their peripheral regions. The images of such disks have recently been computed by Demidova et al. (2013) and Ruge et al. (2015) for the optical and submillimeter spectral ranges, respectively. In this paper, we consider the possibility of applying our models to explain the strong asymmetry in the image of the circumstellar disk around the Herbig Be star LkHα 101 obtained by Tuthill et al. (2002).

[1]The number and quality of protoplanetary disk images will increase rapidly in the coming years owing to the started operation of the ALMA interferometer.

2 The method of calculation

2.1 Protoplanetary disk model

We consider a star with mass M_1 surrounded by a gas–dust disk in which a low-mass companion with mass M_2 moves. We assume that the orbit of the companion is circular and that its plane is inclined to the disk midplane at a small angle α (Fig. 1b). The main parameters of the problem are the star-to-companion mass ratio $q = M_2 : M_1 \leq 0.1$, the orbital inclination to the disk plane α, the effective viscosity of the disk that was defined via the dimensionless speed of sound c expressed in fractions of the Keplerian speed in the companion's orbit (here, we consider the models at $c = 0.05$), and the semi-major axis of the orbit of the companion a.

The calculations of the hydrodynamic flows in the circumstellar disk caused by the companion's motion presented below were performed by the SPH (Smoothed Particle Hydrodynamics) method. The disk mass was assumed to be small compared to the mass of the central star. This allowed the disk selfgravity to be neglected. By analogy with the work by (Artymowicz & Lubow 1996), we chose the initial surface density distribution $\Sigma \approx r^{-1}$, the Shakura–Sunyaev viscosity parameter $\alpha_{ss} = 0.03$, and the relative disk half-thickness $\delta = z/r = 0.1$. In this case, the diffusion time of surface density evolution is $t_\nu \approx 4 \cdot 10^3$ yrs. The implementation of this method is described in detail in Sotnikova & Grinin 2007.

At the initial time, the companion's orbit is inclined to the disk plane at angle α. The time of a "distortion" of the inner part of the circumbinary disk due to the companion–disk interaction can be estimated (Ivanov et al. 1999). At the above parameters, it corresponds to about 10 binary revolutions, but the "distortion" radius can be estimated only numerically. As our calculations show, for the given time it corresponds to $r \approx a$.

Since the large-scale inhomogeneity arises in a comparatively narrow disk region near the companion's orbit, the results of our calculations should not depend strongly on the surface density distribution law. This circumstance also justifies using the isothermal approximation in hydrodynamic calculations. In our simulations, we used 10^5 test particles in a region of radius $6a$. Our simulations showed that the disk is azimuthally homogeneous at a distance of approximately $5a$ and can be smoothly extended. Since the sizes of protoplanetary disks can reach several hundred AU, in our calculations we assume the presence of an outer disk at $r > 6a$.

Our simulations showed that the binary finishes the relaxation stage with the formation of a central gap after 30 revolutions (see Fig. 1a). By this time, it loses about 5% of the particles through their accretion onto the star and the companion. We assume that the distribution of SPH particles at the given time reflects best the distribution of matter in the simulated protoplanetary disk region.

The model calculated in this way was smoothed over the cells of a 3D mesh (with a step of $0.1a$). This procedure allows the influence of random fluctuations in the distribution of SPH particles to be reduced while retaining all details of the flow structure.

In this paper, we do not investigate the evolution of the inclination of the disk or orbit, because the time of our simulations is limited ($t \leq 200P$). It is well known from the studies of similar binaries that the circumbinary disk in binaries with a massive companion is rapidly aligned with the binary orbit under the action of periodic perturbations (see, e.g., Ivanov et al. 1999; Nixon 2012). In contrast, in binaries with a low-mass companion (a planet), the companion's orbit is aligned with the circumbinary disk plane (Xiang-Gruess & Papaloizou 2013). The fact that the inner regions of the circumstellar disks around β Pic and CQ Tau are inclined relative to the periphery suggests that such binaries can exist for a fairly long time.

2.2 Disk illumination by direct stellar radiation

When calculating the surface brightness of the protoplanetary disk, we assumed the dust to be well mixed with the gas. As in previous papers, the opacity κ per gram of matter was taken to be 250 cm^2 g^{-1} (corresponding to the optical properties of circumstellar dust at a wavelength of about 0.2μm; Henning & Stognienko 1996). The dust-to-gas ratio was taken to be the same as, on average, in the interstellar medium, 1 : 100. The particle mass used in the SPH models can be determined by two methods: first, if the accretion rate onto the binary components $\dot{M}_a$ is specified as a parameter of the problem and is compared with the accretion rate of SPH particles, which is calculated during our simulations. Second, the mass of the simulated part of the disk can be specified as a parameter of the problem. In our calculations, the particle mass m_d was $(3-6) \cdot 10^{22}$ g, corresponding to an accretion rate $\dot{M}_a \approx 10^{-9} M \odot \cdot yr^{-1}$ and a mass of the simulated disk region $M_d \approx 3 \cdot 10^{-6} M_\odot$.

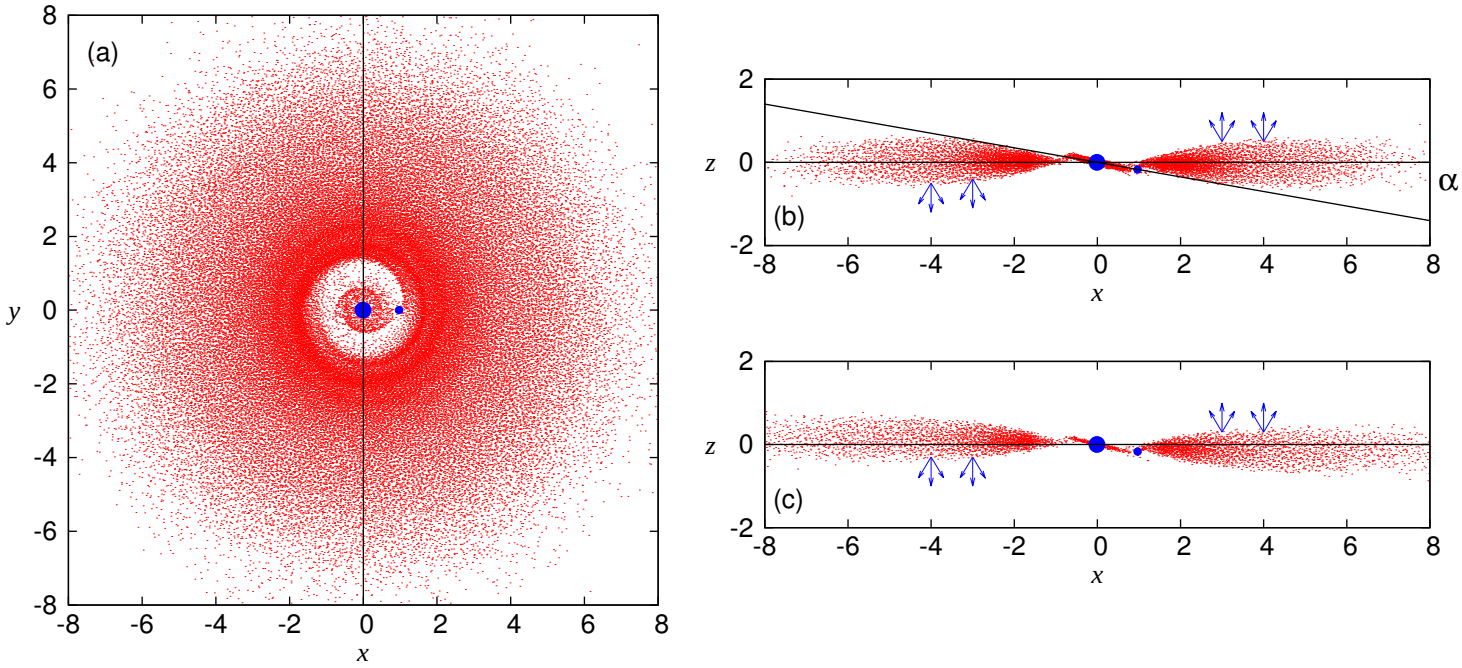

Figure 1: View of the disk after 30 binary revolutions: (a) pole-on view, (b) sections along the y axis, and (c) the same as (b) after 200 binary revolutions. The model: $q = 0.01$ and $\alpha = 10°$ The arrows indicate the disk regions heated by direct stellar radiation, which gives rise to a bright region on the disk. A shadow zone is formed on the opposite side.

To calculate the illumination of the disk by direct stellar radiation, its surface should be described mathematically. For this purpose, the disk plane was divided into cells in radius r and azimuth ϕ (the azimuthal angle is measured from the y axis that coincides with the line of nodes in the direction of the companion's motion, i.e., clockwise). Having calculated the distribution of SPH particles in the disk for each orbital phase and given the particle mass, we find the surface density $\Sigma(r, \phi)$ in each cell. Hence, by assuming the matter in the disk to be distributed according to the barometric law, we obtain the distribution of matter along z at each point r, ϕ:

$$\rho(r, \phi, z) = \rho_0(r, \phi) \cdot e^{-(z/h_0)^2}, \tag{1}$$

Here, h_0 is the density scale height in the disk at point r: $h_0(r) = \sqrt{2}c/\Omega$, where c is the speed of sound in the disk and Ω is the Keplerian angular velocity at this point; the density ρ_0 at $z = 0$ is determined from the relation

$$\Sigma(r, \phi) = \int_{-\infty}^{\infty} \rho(r, \phi, z) dz = \sqrt{\pi}\, h_0(r)\, \rho_0(r, \phi), \tag{2}$$

The disk surface at point r, ϕ was defined in such a way that the optical depth of the disk from the top to point z_1 was equal to unity ($\tau_{z_1} = \kappa \cdot \Sigma_{z_1} = 1$, where Σ_{z_1} is the surface density to level z_1) (Fig. 2). The illumination of each cell on the disk surface by direct stellar radiation was determined from the formula (Tambovtseva et al. 2006).

$$F_s(r, \phi, z_1) = \frac{L_* e^{-\tau(r,\phi,z_1)}}{4\pi(r^2 + {z_1}^2)}\, sin(\gamma), \tag{3}$$

where L_* is the star's luminosity; $\tau(r, \phi, z_1)$ is the optical depth of the dust layer between the star and an arbitrary point on the disk at distance r from the symmetry axis, azimuth ϕ, and height z_1, γ is the angle between the vector connecting the star and the point on the disk surface and the tangent to the disk surface

at this point (for details, see Demidova et al. 2013). The particles in the inner disk region, at $r \leq r_s$, where r_s is the radius of the dust sublimation zone, were not involved in our calculations of the optical depth. We calculated r_s based on Eq. 3 and the Stefan–Boltzmann law $F = \sigma T^4$ at a silicate dust sublimation temperature of 1500 K.

In this paper, we consider a bright Herbig Be star with a mass of $\sim 10 M_\odot$ and a luminosity $L_1 \approx 10^3 L_\odot$. At the mass ratio $q = 0.01$, the companion's mass is $0.1 M_\odot$ and it is an M-type star with a luminosity $L_2 \approx 10^{-3} L_\odot$. We neglected the disk illumination by the companion, because it is negligible compared to the illumination by the central star. However, the companion's luminosity at the highest point of the orbit (above the disk), at the time when it passes near the shadow zone, can exceed the illumination of the shadow zone. Since, however, the companion is near the inner boundary of the shadow zone at this time, this effect can hardly be noticed during observations. The disk heating through viscous dissipation (at the accretion rate $10^{-9} M_\odot$ under consideration) is negligible even near the star and was disregarded in our calculations.

2.3 Allowance for the scattered radiation

The contribution of scattered light to the illumination of protoplanetary disks around young stars typically accounts for a few percent of the stellar radiation. However, scattered light plays a significant role in the illumination of the disk regions into which no direct stellar radiation penetrates. In our calculations, we assumed the scattering layer to be above the disk surface (defined above) at such a distance z from its midplane that $0.1 \leq \tau_z \leq 1$ (Fig. 2). The scattering layer was divided into cells in r, ϕ, and z. The illumination of each volume element with coordinates r', ϕ', z' in this layer was calculated from a formula similar to (3):

$$F_s(r', \phi', z') = \frac{L_* e^{-\tau(r', \phi', z')}}{4\pi(r'^2 + z'^2)}. \quad (4)$$

The disk illumination was then calculated at each point of the surface in the single-scattering approximation by integration over the entire volume of the scattering layer:

$$F_{sc}(r, \phi, z_1) = k_{sc} \int_0^{2\pi} d\phi' \int_{r_s}^{5a} r' dr' \int_{z_1}^{z_2} \frac{F_s(r', \phi', z')}{4\pi |\overrightarrow{\mathbf{d}}|^2} \rho(r', \phi', z')\, f(\theta)\, e^{-\tau(r', \phi', z', r, \phi, z_1)}\, cos\,\xi\, dz'. \quad (5)$$

Here, $\overrightarrow{\mathbf{d}}$ is the vector between the center of the scattering cell and the center of the area on the disk surface with coordinates r, ϕ, z_1 on which scattered light is incident, ξ is the angle between the vector $\overrightarrow{\mathbf{d}}$ and the normal to the disk surface at the area center; k_{sc} is the scattering coefficient, $\tau(r', \phi', z', r, \phi, z_1)$ is the dust optical depth on the ray running away from the scattering cell to the area on the disk surface. We used the Henyey–Greenstein phase function: $f(\theta) = (1 - g^2)/(1 + g^2 - 2g\, cos\theta)^{3/2}$, where g is the asymmetry factor and θ is the scattering angle. The asymmetry factor g and the scattering albedo were taken to be 0.5 (Mathis et al. 1977). Hence, the scattering coefficient is $k_{sc} = 125$ cm^2 g^{-1}.

2.4 Calculation of the disk image

Keeping in mind the application of the results of our calculations to the circumstellar disk of LkHα 101 observed in the K band, we calculated the model images for this photometric band. The total illumination of each cell on the disk surface is $F = F_s + F_{sc}$. By assuming each cell on the disk surface to radiate as a blackbody, we determined the disk temperature as a function of r and ϕ from the Stefan–Boltzmann law: $T = (F/\sigma)^{1/4}$. The luminosity for 1 cm^2 of the disk surface was determined by taking into account the wavelength dependence of the transmission coefficients $f_K(\lambda)$ for the K band of the Johnson 1965 standard photometric system:

$$L_K(r, \phi) = \int_\lambda B_\lambda(T(r, \phi))\, f_K(\lambda) d\lambda. \quad (6)$$

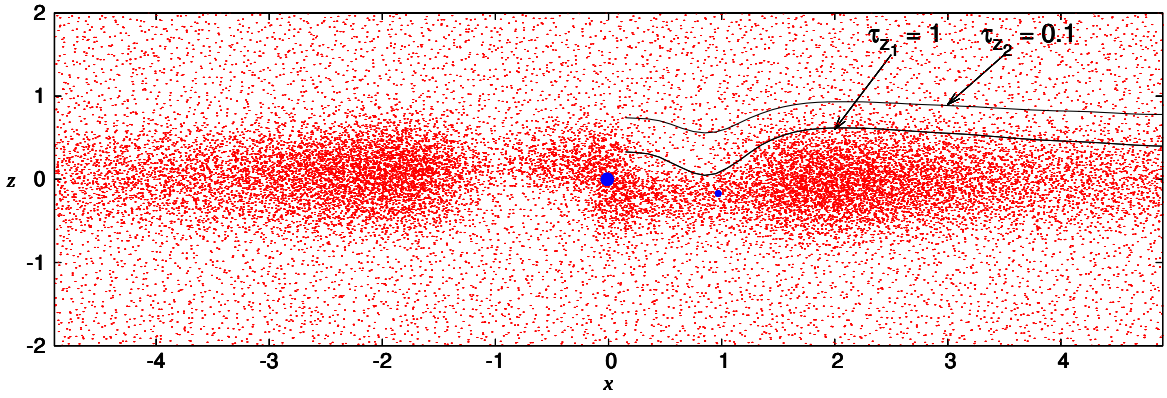

Figure 2: Disk section in the z, x plane in model 1. The companion's orbital radius is taken as unity. We consider the level where the vertical optical depth $\tau_{z_1} = 1$ to be the disk surface and the region between $\tau_{z_1} = 1$ and $\tau_{z_2} = 0.1$ to be the scattering layer.

3 Results

3.1 Model of the Protoplanetary Disk around LkHα 101

LkHα 101 is a young star surrounded by a massive circumstellar disk. Despite the large number of works devoted to this star, its basic parameters are known very inaccurately. For example, there is a spread from 160 (Stine & O'Neal 1998) to 800 pc (Herbig 1971) in the estimated distance D to the object. Tuthill et al. (2002) surmised (by comparing the radio and photometric observations) that LkHα 101 is an early-B star with a mass $M_* \simeq 10 - 20 M_\odot$ and a luminosity $L \simeq (10 - 25) \cdot 10^3 L_\odot$. According to their estimates, the most probable distance to the object is ~ 340 pc. On the other hand, according to Herbig et al. (2004), the star has a strong reddening ($A_v \simeq 10$) and a luminosity ($\geq 8 \cdot 10^3 L_\odot$). They estimated its distance to be ~ 700 pc.

Tuthill et al. (2002) obtained a near-IR image of the disk around Lk Hα 101 (Fig. 3). In its central part, the disk is asymmetric and has the shape of a "horseshoe". Tuthill et al. (2002) explain this asymmetry by assuming the disk to be inclined at a small angle to the plane of the sky. In this case, an observer can see part of the puffed-up inner rim in the sublimation zone of the dust disk located behind the star, while the frontal part of the rim will be shielded by the disk itself. This model has two weak points: first, the disk must be geometrically very thick and, second, the image of a disk inclined to the plane of the sky must have an elliptical shape. However, as can be seen from Fig. 3, the outer boundary of the image is described with a good accuracy by a circumference but not by an ellipse. This suggests that the disk is viewed nearly pole-on.

We calculated the image of the circumstellar disk around LkHα 101 by assuming the star to have a low-mass companion moving in a noncoplanar (relative to the disk) orbit. Since the distance D to the object is known inaccurately and since there is a spread from 160 to 800 pc, we chose two cases: 160 and 340 pc. In the first case, (model 1, $D = 160$ pc), the luminosity of the central star is $L_* = 1300 L_\odot$, the radius of the disk image is $R_d = 7.1$ AU (44 mas), the orbital radius of the companion is $a = 4$ AU, and the radius of the dust sublimation zone is $r_s = 2.4$ AU; in the second case (model 2, $D = 340$ pc), $L_* = 5900 L_\odot$, $R_d = 14.9$ AU, $a = 8.8$ AU, and $r_s = 5.3$ AU. In both cases, the companion-to-star mass ratio is $q = 0.01$ and the orbital inclination is $\alpha = 10°$.

Figure 4 shows K-band images of the circumstellar disk for the two models described above. In each case, the disk is viewed pole-on, but the presence of an inhomogeneity in the distribution of matter in the central part of the disk leads to an asymmetry in the disk illumination by the star. As a result, the disk images resemble a "horseshoe". The presence of a weakly illuminated region on the disk stems from the fact

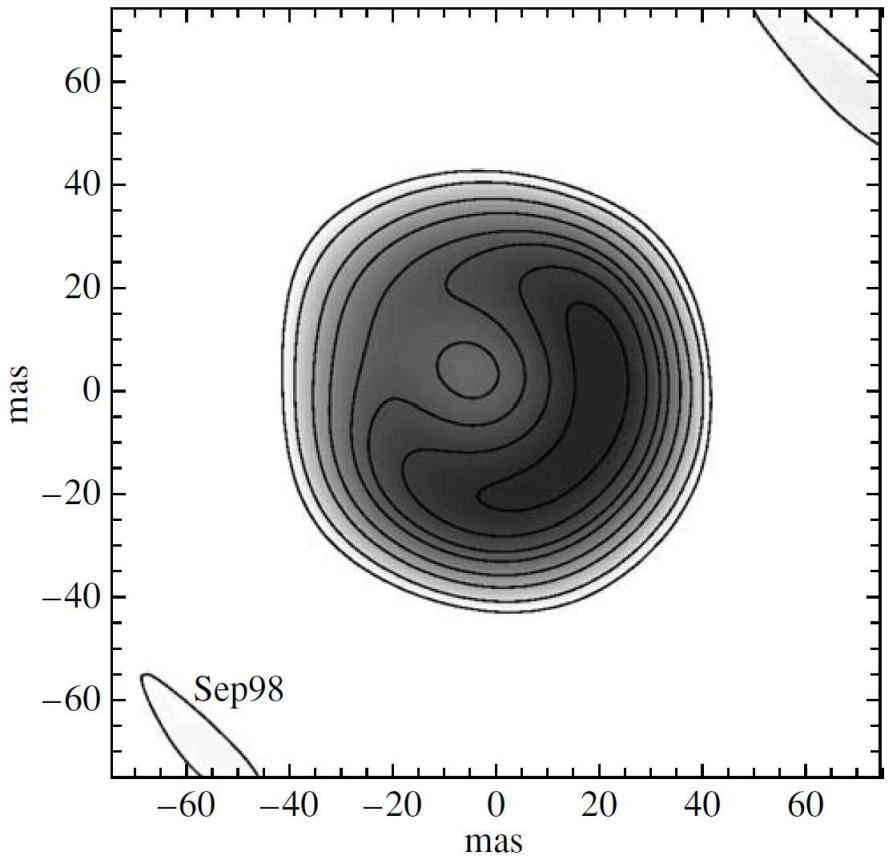

Figure 3: Image of the disk around LkHα 101 in the CH4 filter (2.27 μm) obtained by Tuthill et al. (2002) in September 1998.

that the part of the disk located within the companion's orbit is inclined relative to the midplane of the remaining disk and casts a shadow.

3.2 Influence of the companion's orbital motion

The orbital motion of the companion affects the distribution of matter in the central part of the circumstellar disk and leads to variations in the illumination of its outer part. In the case under consideration, as in our previous paper (Demidova et al. 2013), the illuminated region follows neither the rotation of the companion nor the rotation of the disk itself but only executes small oscillations relative some preferential direction. The sizes of the bright region also slightly change with orbital phase, but the "horseshoe"-shaped image remains approximately in the same disk area (Fig. 5). This peculiarity distinguishes our model from other models in which the inhomogeneities in the disk illumination move across the disk either with the star's rotation period (in the model of a spotted star by Wood & Whitney 1998) or with the companion's orbital period (in the model by Tambovtseva et al. 2006).

In the model with a noncoplanar orbit, the inner disk region precesses (Papaloizou & Terquem 1995; Larwood & Papaloizou 1997). The precession period depends on binary parameters. In our model, the precession period is several hundred orbital periods. Therefore, the influence of this factor on the disk illumination asymmetry can be noticeable only on very long time scales.

3.3 Other objects

LkHα 101 is one of the brightest objects in the near-IR spectral range, because the disk is observed around a very hot star. Similar (in shape) images of circumstellar disks (a "horseshoe"-shaped asymmetry with a circular outer boundary) have recently been observed for other stars in the mid-IR spectral range. These

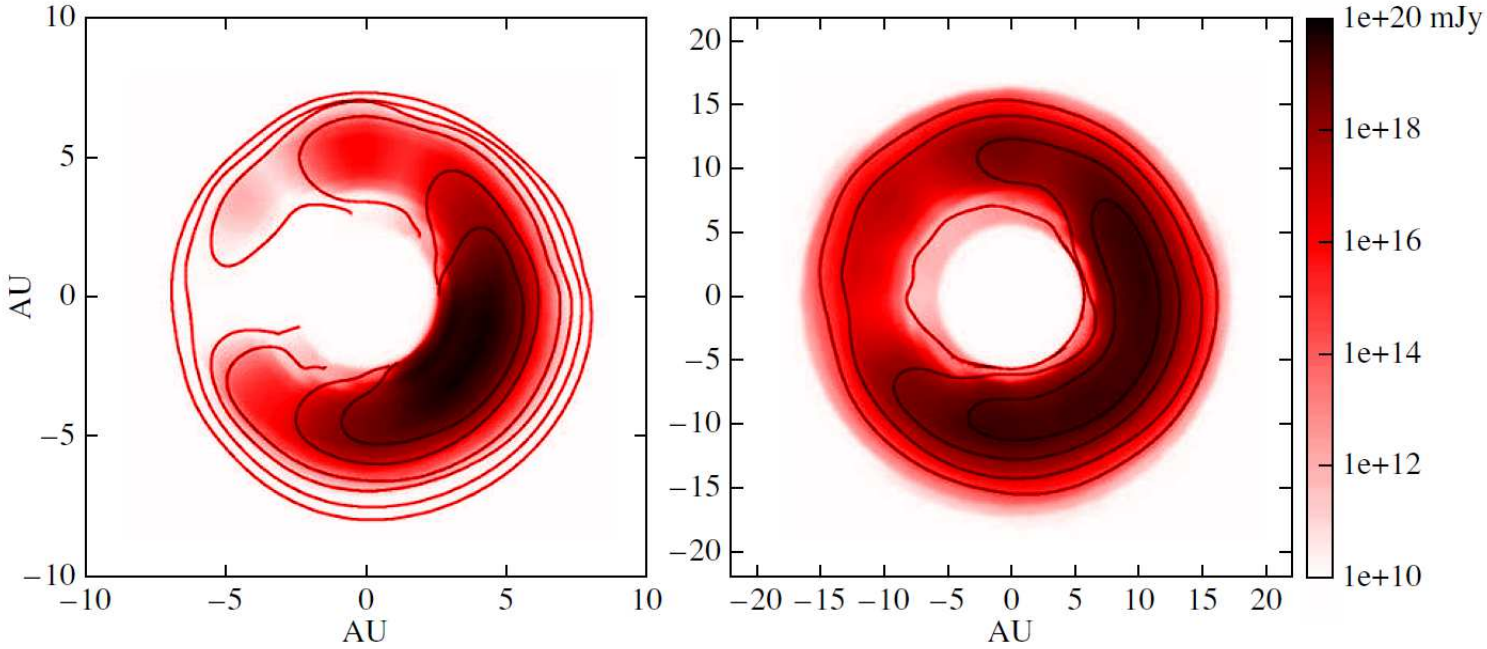

Figure 4: Theoretical image of the protoplanetary disk in the K band (here and below, the color scale corresponds to the disk surface luminosity calculated from Eq. 6): model 1 (left panel) and model 2 (right panel). The radius of the gap in the central part of the image is equal to the radius of the sublimation zone in the model under consideration.

include the disks around the stars HD 169142 and HD 100453 whose images at 12 μm were obtained by Mariñas et al. (2011). There is evidence that HD 100453 has a companion (Chen et al. 2006). The Herbig Ae star HD 142527 is surrounded by a massive gas–dust disk viewed nearly pole-on. Near- IR (Fukagawa et al. 2006) and mid-IR (Fujiwara et al. 2006) observations showed that the image of the disk around this young star has a strong asymmetry similar to that observed for LkHα 101. In addition, there is a matter-free gap in the disk between 30 and 130 AU (Verhoeff et al. 2011). Fukagawa et al. (2006) hypothesize that the gap is formed by a companion moving in an eccentric orbit (see also Biller et al. 2012).

4 Conclusions

The calculations presented here show that the asymmetry in the images of protoplanetary disks can be due to an anisotropic illumination of the disk by the central star. A nonuniform distribution of matter in the central disk region, which affects (via extinction) the propagation of stellar radiation, is responsible for the azimuthally nonuniform illumination. The large-scale inhomogeneity is caused by the perturbations in the disk arising when the companion moves in an orbit that is noncoplanar with the disk. As our calculations showed, an appreciable asymmetry can be caused by a companion whose mass is lower than that of the central star by a factor of 100. The theoretical disk images have a bright "horseshoe"-shaped region with a circular outer boundary (when viewed pole-on). Such disk images agree well with the observational data. The model we considered imposes no constraints on the disk thickness and requires no disk inclination to the plane of the sky.

Tuthill et al. (2002) presented the images of the disk around LkHα 101 obtained at different dates from December 1997 to January 2001. They slightly change with time, but the bright "horseshoe"-shaped region whose position does not change is seen at all dates of observations. In our models, the disk image behaves similarly: the orbital motion of the companion leads only to small oscillations in the positions of the bright region with its overall shape retained. This behaviour of the disk image differs fundamentally for the models of other authors in which the bright and dark regions on the disk follow the rotation of a star with an inhomogeneous surface (Wood & Whitney 1998), or the orbital motion of the companion (Tambovtseva et al.

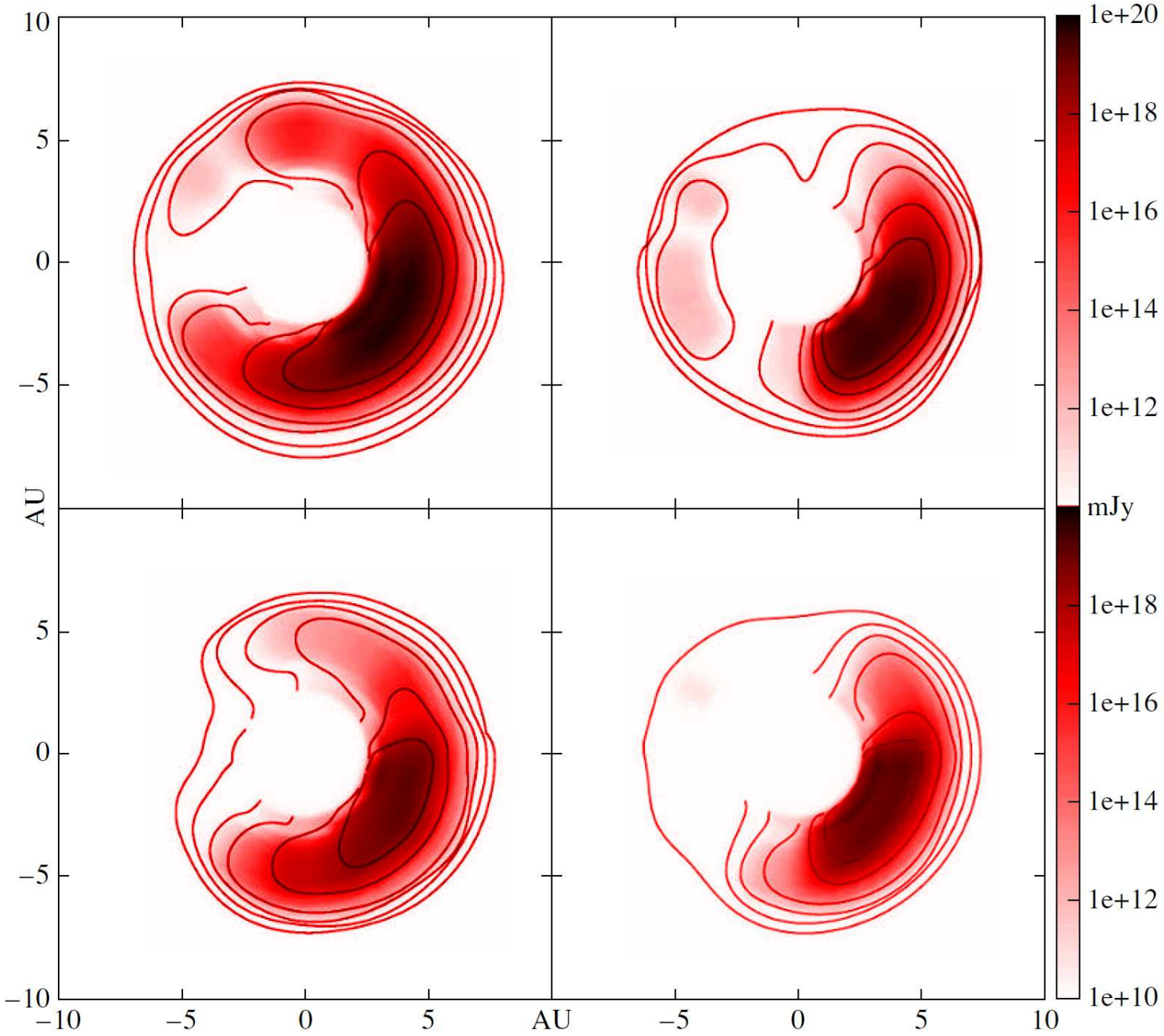

Figure 5: Theoretical images of the protoplanetary disk for model 1 in the K band during one period: from left to right, from top to bottom.

2006), or the motion together with the disk of a giant cyclone (Birnstiel et al. 2013).

Apart from the global asymmetry caused by the orbital inclination of the companion to the disk, the companion's motion gives rise to gas flows and shock waves in the binary's inner regions as well as an accretion disk around the companion and a dusty disk wind. Such structures can give rise to small shadow zones on the disk that will move with the companion's rotation period against the background of the global asymmetry caused by the orbital inclination to the disk.

The question about the evolution of such binaries remained outside the scope of this study, but, as has been pointed out above, the existence of edge-on circumstellar disks in which the inner region is inclined relative to the periphery (β Pic, CQ Tau) suggests that the "twisted" disk can exist for a fairly long time. Our calculations showed that the part of the disk located within the companion's orbit slowly precesses.

However, the precession rate is too low for this effect to be detectable during observations.

It should be emphasized that the model we considered is applicable only to optically thick disks (i.e., in the optical and near-IR ranges). As the radiation wavelength increases, the contrast between the dark (shadow) and bright regions of the disk decreases, but the shape of the asymmetry remains as before. In the submillimeter range, the disk is transparent to radiation and a bright region arises at the location of the shadow zone (the part of the disk heated on the opposite side is transparent, see Fig. 1b). The differences between the disk images in different spectral ranges described above are of interest from the viewpoint of observationally testing the proposed model and deserve a further study.

Acknowledgments. We are grateful to N.Ya. Sotnikova, who provided the software package for hydrodynamic model calculations. This work was supported by a grant from the St. Petersburg Committee for Science and Higher School, Program P21 of the Presidium of the Russian Academy of Sciences, and grant NSh-1625.2012.2.

References

Albrecht, S., Winn, J. N., Johnson, J. A., et al. 2012, ApJ, 757, 18

Artymowicz, P. & Lubow, S. H. 1996, ApJ, 467, L77

Bate, M. R. & Bonnell, I. A. 1997, MNRAS, 285, 33

Bate, M. R., Lodato, G., & Pringle, J. E. 2010, MNRAS, 401, 1505

Biller, B., Lacour, S., Juhász, A., et al. 2012, ApJ, 753, L38

Birnstiel, T., Dullemond, C. P., & Pinilla, P. 2013, A&A, 550, L8

Bitsch, B. & Kley, W. 2011, A&A, 530, A41

Chapillon, E., Guilloteau, S., Dutrey, A., & Piétu, V. 2008, A&A, 488, 565

Chen, X. P., Henning, T., van Boekel, R., & Grady, C. A. 2006, A&A, 445, 331

de Val-Borro, M., Artymowicz, P., D'Angelo, G., & Peplinski, A. 2007, A&A, 471, 1043

Demidova, T. V., Grinin, V. P., & Sotnikova, N. Y. 2013, Astronomy Letters, 39, 26

Demidova, T. V., Sotnikova, N. Y., & Grinin, V. P. 2010, Astronomy Letters, 36, 422

Doucet, C., Pantin, E., Lagage, P. O., & Dullemond, C. P. 2006, A&A, 460, 117

Eisner, J. A., Lane, B. F., Hillenbrand, L. A., Akeson, R. L., & Sargent, A. I. 2004, ApJ, 613, 1049

Fabrycky, D. & Tremaine, S. 2007, ApJ, 669, 1298

Fragner, M. M. & Nelson, R. P. 2010, A&A, 511, A77

Fujiwara, H., Honda, M., Kataza, H., et al. 2006, ApJ, 644, L133

Fukagawa, M., Tamura, M., Itoh, Y., et al. 2006, ApJ, 636, L153

Grady, C. A., Woodgate, B. E., Bowers, C. W., et al. 2005, ApJ, 630, 958

Grinin, V. P., Demidova, T. V., & Sotnikova, N. Y. 2010, Astronomy Letters, 36, 808

Günther, R. & Kley, W. 2002, A&A, 387, 550

Hanawa, T., Ochi, Y., & Ando, K. 2010, ApJ, 708, 485

Hashimoto, J., Tamura, M., Muto, T., et al. 2011, ApJ, 729, L17

Henning, T. & Stognienko, R. 1996, A&A, 311, 291

Herbig, G. H. 1971, ApJ, 169, 537

Herbig, G. H., Andrews, S. M., & Dahm, S. E. 2004, AJ, 128, 1233

Ivanov, P. B., Papaloizou, J. C. B., & Polnarev, A. G. 1999, MNRAS, 307, 79

Johnson, H. L. 1965, ApJ, 141, 923

Kaigorodov, P. V., Bisikalo, D. V., Fateeva, A. M., & Sytov, A. Y. 2010, Astronomy Reports, 54, 1078

Lai, D., Foucart, F., & Lin, D. N. C. 2011, MNRAS, 412, 2790

Larwood, J. D., Nelson, R. P., Papaloizou, J. C. B., & Terquem, C. 1996, MNRAS, 282, 597

Larwood, J. D. & Papaloizou, J. C. B. 1997, MNRAS, 285, 288

Mariñas, N., Telesco, C. M., Fisher, R. S., & Packham, C. 2011, ApJ, 737, 57

Muto, T., Grady, C. A., Hashimoto, J., et al. 2012, ApJ, 748, L22

Nagasawa, M., Ida, S., & Bessho, T. 2008, ApJ, 678, 498

Nixon, C. J. 2012, MNRAS, 423, 2597

Padgett, D. L., Brandner, W., Stapelfeldt, K. R., et al. 1999, AJ, 117, 1490

Papaloizou, J. C. B. & Terquem, C. 1995, MNRAS, 274, 987

Ruge, J. P., Wolf, S., Demidova, T., & Grinin, V. 2015, A&A, 579, A110

Sotnikova, N. Y. & Grinin, V. P. 2007, Astronomy Letters, 33, 594

Stine, P. C. & O'Neal, D. 1998, AJ, 116, 890

Tambovtseva, L. V., Grinin, V. P., & Weigelt, G. 2006, A&A, 448, 633

Thommes, E. W. & Lissauer, J. J. 2003, ApJ, 597, 566

Triaud, A. H. M. J., Collier Cameron, A., Queloz, D., et al. 2010, A&A, 524, A25

Tuthill, P. G., Monnier, J. D., Danchi, W. C., Hale, D. D. S., & Townes, C. H. 2002, ApJ, 577, 826

Verhoeff, A. P., Min, M., Pantin, E., et al. 2011, A&A, 528, A91

Wood, K. & Whitney, B. 1998, ApJ, 506, L43

Xiang-Gruess, M. & Papaloizou, J. C. B. 2013, MNRAS, 431, 1320